Letter

The Unusual Electrochemical and Photophysical Behavior of 2,2‘-Bis(1,3,4-oxadiazol-2-yl)biphenyls, Effective Electron Transport Hosts for Phosphorescent Organic Light Emitting Diodes

Man-kit Leung, Chih-Chiang Yang, Jiun-Haw Lee, Hsin-Hung Tsai, Chi-Feng Lin, Chih-Yen Huang, Yuhlong Oliver Su, and Chi-Feng Chiu

Org. Lett., **2007**, 9 (2), 235-238 • DOI: 10.1021/ol062668+

More About This Article

Additional resources and features associated with this article are available within the HTML version:

- Supporting Information
- Links to the 3 articles that cite this article, as of the time of this article download
- Access to high resolution figures
- Links to articles and content related to this article
- Copyright permission to reproduce figures and/or text from this article

View the Full Text HTML

ORGANIC LETTERS

2007
Vol. 9, No. 2
235−238

The Unusual Electrochemical and Photophysical Behavior of 2,2′-Bis(1,3,4-oxadiazol-2-yl)biphenyls, Effective Electron Transport Hosts for Phosphorescent Organic Light Emitting Diodes

Man-kit Leung,*,†,‡ Chih-Chiang Yang,† Jiun-Haw Lee,*,§ Hsin-Hung Tsai,§ Chi-Feng Lin,§ Chih-Yen Huang,⊥ Yuhlong Oliver Su,*,⊥ and Chi-Feng Chiu||

Department of Chemistry, Institute of Polymer Science and Engineering, Graduate Institute of Electrooptical Engineering, and Department of Electrical Engineering, National Taiwan University, Taipei 106, Taiwan, Department of Applied Chemistry, National Chi Nan University, Nantou 545, Taiwan, and RiTdisplay Corporation, Hsin Chu Industrial Park 30316, Taiwan

mkleung@ntu.edu.tw

Received November 1, 2006

ABSTRACT

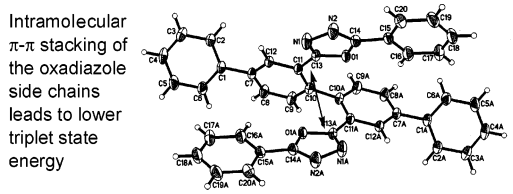

The fluorescence and phosphorescence of 2,2′-bis(5-phenyl-1,3,4-oxadiazol-2-yl)biphenyl shows good spectral matching with the absorption spectra of the MLCT[1] and MLCT[3] transitions of Ir(ppy)$_3$. The red-shift of the 0–0 band in the phosphorescence at 77 K is due to the intramolecular π–π interactions between the oxadiazole side chains. Maximum brightness of 43 000 cd/m^2 with an efficiency of 26 cd/A at 200 cd/m^2 was achieved when BOBP was used as the host material for Ir(ppy)$_3$ in the PHOLED study.

Phosphorescent organic light emitting diodes (PHOLED) are a prime focus of organic light emitting device (OLED) research due to their high light-emitting efficiency.[1] The light emissive mechanism involves triplet excitons that might be self-quenched through triplet−triplet annihilation. Therefore, a host matrix for separation of the phosphorescent materials is usually required.[2] The family of hole-transport carbazoles,[3] such as 4,4′-(bis(9-carbazoyl))biphenyl (CBP),[2] and arylsilane[4] derivatives has attracted a lot of attention due to the compound's low HOMO and large band gap. However, electron transport materials for use as host for the phosphorescent dyes are less common.[5]

1,3,4-Oxadiazoles (OXDs) are electron transport compounds that have been widely used in OLED.[6] However, the use of OXDs as hosts for PHOLED is rare.[7] The basic skeleton of 2,2′-bis(5-phenyl-1,3,4-oxadiazol-2-yl)biphenyl

† Department of Chemistry, National Taiwan University.
‡ Institute of Polymer Science and Engineering, National Taiwan University.
§ Graduate Institute of Electrooptical Engineering and Department of Electrical Engineering, National Taiwan University.
⊥ Department of Applied Chemistry, National Chi Nan University.
|| RiTdisplay Corporation.

(1) (a) Baldo, M. A.; O'Brien, D. F.; You, Y.; Shoustikov, A.; Sibley, S.; Thompson, M. E.; Forrest, S. R. *Nature* **1998**, *395*, 151. (b) O'Brien, D. F.; Baldo, M. A.; Thompson, M. E.; Forrest, S. R. *Appl. Phys. Lett.* **1999**, *74*, 442.

(2) Baldo, M. A; Lamansky, S.; Burrows, P. E.; Thompson, M. E.; Forrest, S. R. *Appl. Phys. Lett.* **1999**, *75*, 4.

(3) (a) Shih, P.-I.; Chiang, C.-L.; Dixit, A. K.; Chen, C.-K.; Yuan, M.-C.; Lee, R.-Y.; Chen, C.-T.; Diau, E. W.-G.; Shu, C.-F. *Org. Lett.* **2006**, *8*, 2799. (b) Wong, K. T.; Chen, Y.-M.; Lin, Y.-T.; Su, H. C.; Wu, C.-c. *Org. Lett.* **2005**, *7*, 5361. (c) Brunner, K.; van Dijken, A.; Börner, H.; Bastiaansen, J. J. A. M.; Kiggen, N. M. M.; Langeveld, B. M. W. *J. Am. Chem. Soc.* **2004**, *126*, 6035. (d) Chen, Y.-C.; Huang, G. S.; Hsiao, C.-C.; Chen, S.-A. *J. Am. Chem. Soc.* **2006**, *128*, 8549.

(4) Ren, X.; Li, J.; Holmes, R. J.; Djurovich, P. I.; Forrest, S. R.; Thompson, M. E. *Chem. Mater.* **2004**, *16*, 4743.

10.1021/ol062668+ CCC: $37.00
Published on Web 12/16/2006

(BOBP) (**3**) attracts us due to the scissor-like conformation with a C_2 rotational axis perpendicular to the long axis of the biphenyl unit.[8] The non-coplanar geometry of the molecule reduces the intermolecular $\pi-\pi$ stacking and retards the nucleation in the crystallization process.

In addition, we are interested in studying BOBPs because various BOBPs can be prepared readily under mild conditions. The key intermediate **4** containing two iodo groups at the 4 and 4′ positions provides a good entry to a variety of BOBPs. Moreover, although the non-coplanar conformation of the biphenyl core would lead to smaller conjugative π-orbital overlapping between two OXD units, the effects of the scissor-like structure on the fluorescent and phosphorscent behavior are unknown and therefore worth investigating.

The syntheses of BOBPs **5**−**13** were started from **4**.[9] Transformation of **1** and **2** into the corresponding OXDs was performed by using a sequence reaction of hydrazide formation, acylation, and dehydration to give **3** and **4**, respectively, in 50% and 55% overall yields.[10] Diiodide **4** was further converted to **5**−**11** under the Suzuki coupling conditions, or to **12**−**13** under the Ullman conditions.[11] Besides, other OXDs including **DPO**, **PBD**, and **TPOB** were used as references for comparison.[12]

Scheme 1. Synthetic Pathways for BOBPs **3** and **5**−**13**

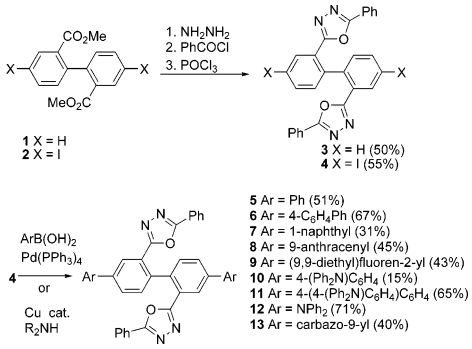

Cyclic voltammetric (CV) study of BOBPs: The $E_{1/2}^{red}$ of (−1.90, −2.14), −2.02, and −1.86 for **3**, **DPO**, and **PBD**, respectively, were close while these values were much higher than the first $E_{1/2}^{red}$ of −1.57 V for the **TPOB**, implying that **3** is less conjugated than **TPOB** and is more **DPO**-like. However, the splitting of the reduction waves of **3** and **5**−**13** reflected that electronic couplings between the OXD side chains are significant.

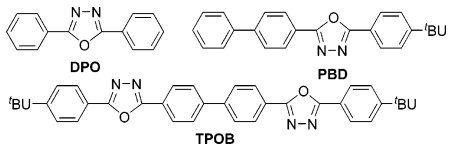

Substituent electronic effects on the reduction processes were small. The first half-reduction potentials $E_{1/2}^{red}$ of the studied BOBPs **5**−**13** were confined in a narrow region of −1.71 to −1.85 V. Introduction of highly electron-donating substituents such as Ph_2N- on the biphenyl core did not significantly retard the reduction, indicating that the substituent electronic effects on the LUMO of BOBPs were small. These results implied that the negative charges of the corresponding radical anions and dianions might mainly locate at the OXD moieties rather than on the biphenyl core (Scheme 2).

Scheme 2. $\pi-\pi$ Interactions between the OXD Side Chains

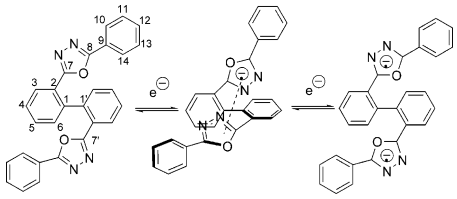

The splittings of the reduction potentials ($\Delta E_{1/2}^{red}$), defined as the $E_{1/2}$ difference between the first two waves, were quite regular, around 0.1−0.2 V. The nearly identical potential splitting suggested that the electronic repulsions between the negative charges of $BOBP^{2-}$ were similar in all cases. The repulsive electronic coupling may originate either from through bond or through space interactions. Our X-ray crystallographic studies suggested that the scissor-like biphenyl conformation allowed π-stacking between the facing OXD units.

X-ray crystallographic characterization of BOBPs: Single crystals of **3**[13] and **5** were successfully prepared from MePh while **6** and **13** were prepared from $CHCl_3$. The ORTEPs of **5** and **13** are shown in Figure 1. The dihedral angles of the biphenyl cores were measured as 85.9°, 74.4° ($C_{11}-C_{10}-C_{10A}-C_{11A}$), 59.2°, and 58.3° ($C_{17A}-C_{16A}-C_{16}-C_{17}$), respectively. The stacking of the OXD rings with a short distance (Å) of 3.82, 3.61, 3.22, and 3.11 between the biphenyl linked OXD carbon atoms was observed. The variation of the $\pi-\pi$ stacking may also be affected by packing effect. The close distance between the OXD units makes the through-space interactions feasible and therefore the first reduction step was stabilized, leading to the splitting of the reduction waves (Scheme 2).

Thermal properties of BOBPs: In the thermal analyses, polycrystalline samples of BOBPs were first melted at high temperature to give isotropic liquids. Fast cooling of the samples gave amorphous glasses that were further analyzed. The

(5) Inomata, H.; Goushi, K.; Masuko, T.; Konno, T.; Imai, T.; Sasabe, H.; Brown, J. J.; Adachi, C. *Chem. Mater.* **2004**, *16*, 1285.
(6) Hughes, G.; Bryce, M. R. *J. Mater. Chem.* **2005**, *15*, 94.
(7) Adachi, C.; Baldo, M. A.; Forrest, S. R.; Thompson, M. E. *Appl. Phys. Lett.* **2000**, *77*, 904.
(8) Eliel, E. L.; Wilem, S. *Stereochemistry of Organic Compounds*; Wiley: New York, 1994; p 1148.
(9) Surry, D. S.; Su, X.; Fox, D. J.; Franckevicius, V.; Macdonald, S. J. F.; Spring, D. R. *Angew. Chem., Int. Ed.* **2005**, *44*, 1870.
(10) Lucas, H. J.; Kennedy, E. R. *Organic Syntheses*; Wiley: New York, 1943; Collect. Vol. II, p 351.
(11) (a) Gilman, H.; Honeycutt, J. B., Jr. *J. Org. Chem.* **1957**, *22*, 226. (b) Zhang, H.; Cai, Q.; Ma, D. *J. Org. Chem.* **2005**, *70*, 5164.
(12) Naito, K.; Watanabe, Y.; Egusa, S. *Jpn. J. Appl. Phys.* **1999**, *38*, 2792.
(13) Baumer, V. N.; Doroshenko, A. O.; Verezubova, A. A.; Ptyagina, L. M.; Kirichenko, A. V.; Ponomarev, O. A. *Khim. Geterotsikl. Soedin.* **1996**, *7*, 984.

Table 1. Electrochemical Data, Thermal Stability, and Photophysical Data for BOBPs and the OXD References

	$E_{1/2}^{red}$ (V)[a]					thermal analysis[d]			photophysical data[e]			
OXD	E_1	E_2	E_3	$\Delta E_{1/2}^{red}$	$E_{1/2}^{ox}$ [b]	T_g	T_c	T_d	A, λ_{max} (ϵ, 10^4)	λ_{max}(Fl)	λ_{max}(Ph)	ΔE_{S-T} (eV)[f]
3	−1.90	−2.14		0.24		44.6	97.4	313	283 (6.20)	367	455	1.04
5	−1.79	−1.95		0.16		85.8	159.1	375	268 (5.19)	392	454	0.72
6	−1.76	−1.90		0.14		113.2	183.0	408	289 (9.28)	408	490	0.67
7	−1.80	−1.97		0.17		107.2		398	289 (3.19)	406	499	0.91
8	−1.72	−1.87	−2.03	0.15	1.33[c]	151.4		401	292 (3.11), 389 (1.95)	420		
9	−1.79	−1.93		0.14		123.1	202.0	411	295 (5.93), 320 (5.15)	415	493	0.68
10	−1.80	−1.94		0.14	1.15	124.0	-	418	290 (4.91), 348 (2.94)	475	495	0.41
11	−1.77	−1.91		0.14	1.09	145.4	236.2	440	283 (6.91), 356 (4.96)	482	515	0.49
12	−1.85	−2.02		0.19	1.28	99.8	-	400	291 (6.29), 379 (0.46)	474	511	0.35
13	−1.72	−1.92		0.20	1.55	139.5	207.0	412	288 (6.40), 340 (1.25)	439	455	0.39
TPOB	−1.57	−1.81		0.24					327 (5.96)	370	417	0.36
DPO	−2.02								283 (2.18)	346	414	0.65
PBD	−1.86								306 (2.58)	365	414	0.34

[a] By CV in DMF, with Bu_4NClO_4 (0.1 M) as supporting electrolyte vs Ag/AgCl. The scan rate was 100 mV/s. [b] In CH_2Cl_2. [c] Irreversible waves. [d] Scan rate: 10 deg/min. [e] Measured in $CHCl_3$. [f] The singlet−triplet energy difference.

glass-transition temperatures (T_g) and the temperature at 5% weight loss (T_d) in TGA are listed in Table 1 for comparison.

When the glassy samples were heated, glass transitions were observed for all BOBPs. For some BOBPs with higher crystallinity, crystallization took place upon further heating above the T_g. BOBPs **5** and **6** having a longer phenylene chain showed higher T_g and T_c. A linear correlation between T_g versus crystallization temperature (T_c) was observed, suggesting that the rate of nucleation and crystallization in the amorphous glass is correlated to the energy barrier of the molecular motion in the glassy matrix. Introduction of laterially expanded substituents such as naphthyl or anthracenyl groups in **7**, **8**, or relatively flexible diphenylamino groups in **10** and **12** at the terminal of the biphenyl core retarded the crystallization process. And no crystallization took place from the corresponding amorphous glasses when heated after T_g. On the other hand, **11** having a long oligophenylene axis or **13** having relatively rigid carbazole substituents showed T_c at high temperature.

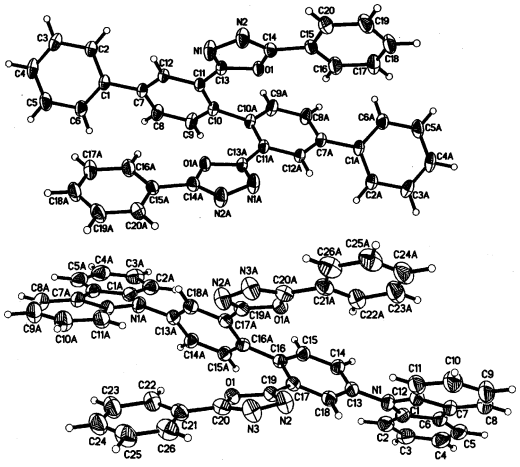

Figure 1. ORTEP's of **5** (upper) and **13** (lower)

Photophysical properties of BOBPs: The UV−vis absorption, fluorescent, and phosphorescent data are summarized in Table 1. Aryl-substituted **5**−**9** showed fluorescent emission peaked at the region of 367−420 nm. On the other hand, for the amino-substituted BOBPs **10**−**12**, significant red-shift of the fluorescent (Fl) emissions to the region of 474−482 nm was observed. The degree of the red-shift was solvent dependently. The λ_{max} of the emissions of **12** in MePh, THF, EtOAc, CH_2Cl_2, and MeCN were 459, 464, 470, 474, and 482 nm, respectively. The fluorescence quantum yields[14] dropped from 0.52 in THF to 0.30 in MeCN. We attribute the red-shift phenomena to the charge-transfer characters of the corresponding S_1-S_0 transition.[15]

The spectra of **3**, **DPO**, and **PBD** are shown in Figure 2.

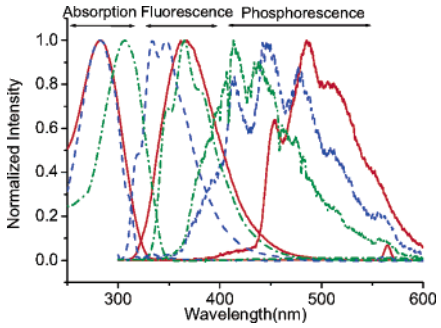

Figure 2. Absorption and emission spectra of **3** (red solid line), **DPO** (---), and **PBD** (-•-).

While the absorption bands of **3** and **DPO** at 280 nm were almost identical, the absorptions of **PBD** and **TBOP** were

(14) Determined by comparison against coumarin C1 as the standard in THF and MeCN. For reference, see: Rusalov, M. V.; Druzhinin, S. I.; Uzhinov, B. M. *J. Fluorescence* **2004**, *14*, 193.

(15) Lakowicz, J. R. *Principles of Fluorescence Spectroscopy*, 2nd ed.; Kluwer-Plenium: New York, 1999; pp 186−187.

respectively red-shifted by 23 and 44 nm, indicating that the conjugation between two OXD moieties of **3** is small. On the other hand, the structureless fluorescent emission of **3** was red-shifted to 367 nm, by 21 nm with respect to **DPO**. We attribute this to the structural relaxation of the S_1 state of **3**, from the scissor-like conformation to the coplanar conformation with better π-conjugation that leads to the red-shift in emission. Indeed, the structural relaxation was inhibited when **3** was frozen in an EtOH matrix at 77 K to give the fluorescence back to a **DPO**-like fine pattern, with the λ_{max} at 353 nm.

To be an appropriate host material, the host should have a triplet energy (E_T) higher than the phosphorescent emitter to prevent the triplet energy back-transfer from the emitter to the host.[4] Although endothermic energy transfer (ET) has been known in literature, an exothermic ET process usually has the advantage of higher efficiency. In our design, one critical issue is whether the E_T of BOBPs are high enough so that the criteria of the exothermic ET process would hold. Phosphorescent (Ph) experiments at 77 K in EtOH or THF revealed that most of the aryl-substituted BOBPs exhibited a 0−0 band at the region of 450−490 nm, corresponding to an energy gap of 2.76−2.53 eV. The results indicated that the family aryl-substituted BOBP are suitable host materials for green-light triplet emitters. On the other hand, due to the low E_T level of the anthracenyl,[16] the triplet emissions of **8** were quenched. Resembling the fluorescent properties, the amino substituted **10**−**12** showed significant red-shift in the phosphorescent emission. However, the red-shift effect on **13** is much less, making it a suitable host for green PHOLED.

Noteworthy to point out is the significant red-shift of phosphorescent emissions of **3** with respect to that of **PBD**, **TPOB**, and **DPO**. Since **3** was frozen in EtOH glass at 77 K during experiment, one may expect that the structural relaxation after excitation would be minimal and the scissor-like conformation would be maintained. Therefore, the red-shift phenomenon could not be simply explained by increasing π-conjugation at the T_1 state. We tentatively attribute this to the through-space interactions between the OXD side chains.

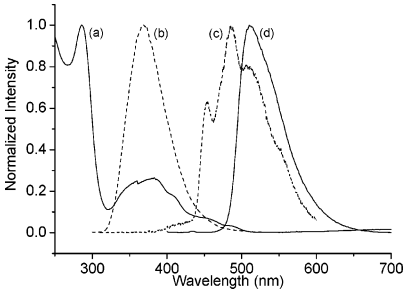

Figure 3. Spectral matching between **3** and $Ir(ppy)_3$: (a) absorption spectrum of $Ir(ppy)_3$, (b) thin-film fluorescent emission of **3**, (c) phosphorescent emission of **3** at 77 K, and (d) phosphorescent emission of $Ir(ppy)_3$.

Figure 3 shows the thin-film fluorescent and the low-temperature phosphorescent spectra of **3** and the absorption and photoluminescent spectra of $Ir(ppy)_3$. Good spectral overlapping of the fluorescent and phosphorescent spectra of **3** with the MLCT[1] and MLCT[3] absorption of $Ir(ppy)_3$ suggested that the energy transfer from **3** to $Ir(ppy)_3$ is effective and exothermic.[17]

The performance of the BOBPs as host in the phosphorescent OLED: To evaluate the performance of the BOBPs as the host material for PHOLED, a device of ITO (1100 Å)/α-NPB (400 Å)/BOBP−$Ir(ppy)_3$(9 wt %) (300 Å)/BCP (100 Å)/$BeBq_2$ (300 Å)/LiF (12 Å)/Al (1000 Å) was employed for the preliminary study (Figure 4). BOBP **3** was

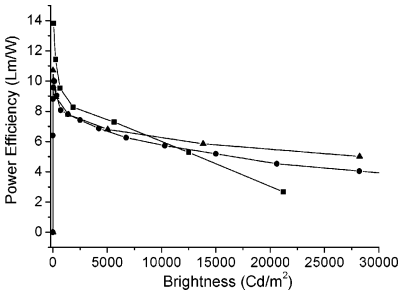

Figure 4. Power efficiency versus brightness of the PHOLED devices of **3** (■), **13** (●), and CBP (▲).

first selected as the host material to test in our study. The luminescence current efficiency (CE) of 26 cd/A was found at the brightness of 200 cd/m^2. A maximum brightness of 43 000 cd/m^2 was achieved. Although the CE is slightly lower than the PHOLED with CBP as the host, in which a CE of 28.6 cd/A was found,[2] the turn-on voltage of the BOBP device is much lower so that the power efficiency is 3 Lm/W higher. The lifetime of the PHOLED device was 2.5 times longer than the CBP one in the accelerated lifetime tests. Although using the ambipolar host **13** for PHOLED only give rise to a CE of 14 cd/m^2, the power efficiency of the PHOLED can be maintained high at high brightness output.

In summary, the through-space interactions between the OXD side chains would lead to unusual red-shift of the phosphorescence of BOBPs. Due to the well-matched spectral properties of **3** and $Ir(ppy)_3$, **3** was found a good electron transport host for the $Ir(ppy)_3$ emitter in PHOLED applications.

Acknowledgment. We thank the Thematic Project of Academia Sinica and the National Science Council of Taiwan for partial financial support.

Supporting Information Available: Preparation procedures, NMR (^{1}H, ^{13}C), absorption and emission spectra, CV of **3** and **5**−**13**, and CIF files for **3**, **5**, **6**, and **13**. This material is available free of charge via the Internet at http://pubs.acs.org.

OL062668+

(16) Carmichael, I.; Hug, G. L. In *Handbook of Organic Photochemistry*; Scaiano, J. C., Ed.; CRC: Boca Raton, FL, 1989; Vol. 1, p 377.

(17) Xie, H. Z; Liu, M. W.; Wang, O. Y.; Zhang, X. H.; Lee, C. S.; Hung, L. S.; Lee, S. T.; Teng, P. F.; Kwong, H. L.; Zheng, H.; Che, C. M. *Adv. Mater.* **2001**, *13*, 1245.